Seismic pore pressure prediction with uncertainty using a probabilistic mechanical earth model

P.M. Doyen, A. Malinverno, R. Prioul, P. Hooyman & S. Noeth, Schlumberger,*
L. den Boer & D. Psaila, WesternGeco, C.M. Sayers, T.J.H. Smit, C. van Eden & R. Wervelman, Shell Intl.E&P *(* formerly of Schlumberger)*

2004 CSEG National Convention

Summary

We propose a methodology to propagate uncertainties in seismic pore pressure prediction using a 3-D Probabilistic Mechanical Earth Model (P-MEM). An extended form of Bowers formula is used to link pore pressure to seismic velocity, overburden stress, porosity and clay volume. Probability Distribution Functions (PDFs) for all input variables are stored as attributes in the 3-D MEM. An output PDF for pore pressure is then calculated point by point in the 3-D model, using either a linearized Gaussian approximation or a sequential stochastic simulation approach that fully accounts for nonlinearities in the velocity to pore pressure transform and spatial correlation between the different input variables. The linearized and stochastic approaches are compared in the context of a seismic pore pressure prediction study involving overpressured reservoir sands.

Introduction

Accurate knowledge of pore pressure is a key requirement for safe well planning in overpressured formations. Pre-drill pore pressure predictions are often obtained from seismic velocities, using an empirical velocity to pore pressure transform. Seismic-based pore pressure calculations are best done with the help of a 3-D Mechanical Earth Model (MEM), as illustrated by Plumb et al. (2000). This subsurface model couples the 3-D seismic data with a numerical representation of the state of stress, the lithology, porosity, fluid content and mechanical properties of the rock strata penetrated during the drilling process. In the context of a MEM, the velocity to pore pressure transform is frequently applied in a deterministic manner with no uncertainty quantification. This means that expensive drilling decisions are often done without adequate risk assessment.

Here we propose a methodology to propagate uncertainties in pore pressure prediction workflows using a probabilistic MEM. At each point in the 3-D model, we store PDFs for all input parameters and rock properties required in the velocity to pore pressure transform. Given PDFs on the input attributes, we calculate an output PDF for pore pressure at each location, using either a linearized approximation or a stochastic simulation approach. The probabilistic MEM may be used to assess drilling risks by calculating for example the probability that pore pressure exceeds some critical level above which drilling becomes too risky.

Methodology

Following Sayers et al. (2003), we start from an expression linking P-wave velocity, V, to pore pressure, P, overburden pressure, S, porosity, ϕ, and clay content C:

$$V = a_1 - a_2\phi - a_3C + a_4(S-P)^{a_5} \qquad (1)$$

where the coefficients a_i have been obtained by well calibration. This relation between effective pressure, $S-P$, and velocity is equivalent to the model proposed by Bowers (1995) with the zero-stress velocity V_o set to $a_1 - a_2\,\phi - a_3C$ in order to account for variations in porosity and lithology. We can invert this equation to obtain an expression for the pore pressure:

$$P = S - \left[\frac{1}{a_4}\left(V - a_1 + a_2\phi + a_3C\right)\right]^{\frac{1}{a_5}} \qquad (2)$$

Equation (2) may be applied point-by-point in a 3-D MEM, assuming that a velocity cube has been obtained by seismic inversion and that porosity and clay content have been interpolated from well data. In practice, the velocity to pore pressure transform must be calibrated for each formation and fluid type. The overburden pressure, S, required in the calculation of P can be obtained from:

$$S(z) = g\int_0^z \rho(u)\,du \qquad (3)$$

where z is the vertical depth and ρ is the density of the fluid saturated rock. In practice, the integral is calculated from a density cube obtained by log interpolation.

Our goal is to quantify uncertainty in pore pressure prediction given uncertainties in the variables on the right-hand side of equation (2). To start, collect all the uncertain variables in a vector x:

$$x = \left[a_1\, a_2\; a_3\, a_4\, a_5\; \phi\; C\; S\; V\right] = \left[x_1 \quad \ldots \quad x_9\right] \qquad (4)$$

and assume that the uncertain variables x_i, i = 1, …, 9, are each characterized by a Gaussian PDF with mean $\hat{x}_i$ and variance var[x_i]. We then rewrite equation (2) generically by expressing the pore pressure P as a function g of the uncertain parameter vector x; i.e., $P = g(x)$. Given Gaussian PDFs for the input variables x_i, we want to calculate an output PDF for P, which is a specified function of the input variables.

Linearized Approximation. In general, the output PDF for P will not be Gaussian because the function g linking pressure to velocity (equation 2) is nonlinear. However, the output PDF can be approximated by a Gaussian distribution via linearization. Consider a Taylor series expansion of g around the mean point $\hat{x}$, keeping only the first order terms to define P_{est} as a linear function of the uncertain input variables:

$$P_{est}(x) \approx g(\hat{x}) + \sum_i \left.\frac{\partial g}{\partial x_i}\right|_{x=\hat{x}} (x_i - \hat{x}_i) \qquad (5)$$

It is easy to demonstrate (Granger, Morgan and Henrion, 1990) that P_{est} has a Gaussian distribution with mean given by:

$$\hat{P}_{est} = g(\hat{x}) \qquad (6)$$

and variance equal to:

$$\mathrm{var}[P_{est}] = \sum_i \left(\frac{\partial g}{\partial x_i}\right)^2 \mathrm{var}[x_i] + \sum_i \sum_{j \neq i} \frac{\partial g}{\partial x_i} \frac{\partial g}{\partial x_j} \mathrm{cov}[x_i, x_j] \qquad (7)$$

where the partial derivatives are evaluated at the mean vector $\hat{x}$. Equation (6) states that the first order estimate of the mean pore pressure is obtained by evaluating the function g at the mean value of each uncertain input variable. Equation (7) shows that a linear estimate of the variance of the pore pressure is obtained as a weighted sum of the variances and covariances of the input variables, with weights representing the sensitivity of the output to the different uncertain inputs. In general, the second term in equation (7) cannot be ignored for input variables such as velocity, porosity and clay content that are significantly correlated.

We will apply equations (6) and (7) to calculate a best first order estimate of P and the uncertainty in this estimate. In practice, this calculation is performed point by point in the 3-D P-MEM, with a Gaussian PDF specified at each location for all uncertain input variables. Input PDFs for porosity, clay content, overburden pressure and seismic velocity are spatially variable, while PDFs for the uncertain coefficients a_i are assumed to be spatially invariant. In what follows, we will denote the spatially variable mean of an input x_i by $\hat{x}_i(u)$, with u representing the coordinates of one point in the 3-D model. Similarly, the spatially variable standard deviation of x_i (square root of var[x_i]) will be denoted by $\sigma_i(u)$. The Gaussian PDFs for the input variables are therefore defined at each point as N[$\hat{x}_i(u)$, $\sigma_i(u)$]. In practice, the means and variances of some of the input distributions will be obtained by 3-D kriging, as shown in the example below.

Stochastic Simulation. The linearized method approximates the output PDF for P by a Gaussian distribution. In reality, even with Gaussian inputs, the output PDF may deviate from normality because the velocity to pore pressure transform (equation 2) is nonlinear. As we will see, statistics depending on the tails of the output PDFs, such as "exceedence" probabilities may be poorly estimated with a Gaussian model. To overcome this problem, a stochastic simulation approach was applied. The simulation procedure consists of the following steps: (1) draw values at random from the PDFs specified for the uncertain input variables, (2) evaluate the model function g for each realization of the random input vector x and (3) approximate the PDF of the output variable P from the histogram of the simulated model outcomes.

In comparison to traditional Monte Carlo simulation, several additional aspects need to be considered in the context of a 3-D P-MEM. First, the input PDFs defined for the same variable at different points in the 3-D model may not be sampled independently. Instead, spatially correlated realizations must be generated for each input attribute. Following Samson et al. (1996), a 3-D simulation of a Gaussian input variable, $x_i^s(u)$, is obtained by adding a spatially correlated Gaussian error field, $\varepsilon_i(u)$, to the mean field $\hat{x}_i(u)$, defined at each location u in the 3-D model:

$$x_i^s(u) = \hat{x}_i(u) + \sigma_i(u)\,\varepsilon_i(u) \qquad (8)$$

In (8), the normalized N(0,1) error field, ε_i, is scaled by the spatially variable standard deviation of the input variable x_i. Fast simulations of the correlated error field are generated using the FFT-MA method (Le Ravalec et al., 2000).

In addition to spatial correlation, a second important aspect of the simulation procedure is that local correlations between the different input variables must be reproduced. This is achieved by sequential simulation of the correlated attributes. For example, we first simulate velocity. Next, we simulate porosity conditional on the co-located simulated V value. Finally, we simulate the clay content input variable locally conditional on both previously simulated values of ϕ and C. A simple Bayesian updating rule (Doyen et al., 1996) is used to calculate the required conditional distributions.

Example

The concept of P-MEM was applied to estimate uncertainty in seismic pore pressure prediction for a deep and highly overpressured reservoir. Seismic velocities over the reservoir interval (Figure 1) have been estimated using reflection tomography. As shown by Sayers et al. (2003), significant lateral velocity variations are observed that relate to changes in effective stress as well as variations in clay content and porosity within the reservoir. Equation (2) was used to estimate pore pressure and associated uncertainty starting from Gaussian PDFs for all input variables specified in equation (4). Means and variances for the PDFs were stored at each cell of a 3-D corner point grid constructed over the reservoir layer. The inverted tomographic velocities define the mean velocity field while the variance field was estimated by assuming a 10% relative error, based on a comparison between seismic velocities and upscaled sonic logs at the wells.

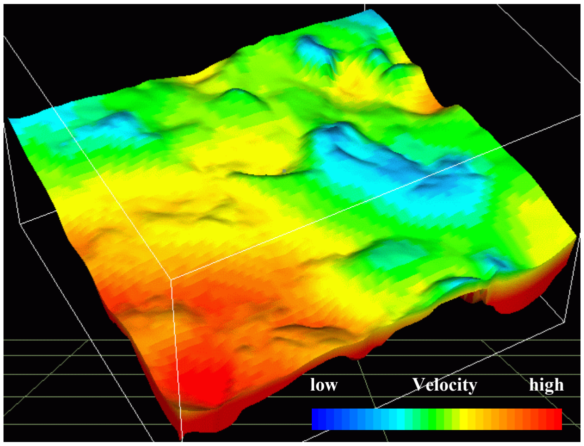

Figure 1. Velocity distribution in the reservoir layer obtained by tomographic inversion. Velocities vary linearly with depth as $V(z) = V_0 + k\,z$, with a constant gradient k and laterally variable V_0.

Mean values for C and ϕ were determined in each cell of the model from 3-D kriging interpolation of log data at 21 wells. The corresponding variances were assigned from the predicted kriging errors. A density cube was constructed by kriging the log data. The input mean field for the overburden pressure, S, was then calculated by vertical integration of the kriged density cube. Approximate overburden pressure errors could be calculated by simply summing the density kriging errors and ignoring correlations between the errors. However, this procedure significantly underestimates the overburden pressure errors because kriging errors tend to be positively correlated. Instead, the variance field for S was calculated from multiple 3-D density simulations that were integrated to obtain an equivalent number of overburden pressure simulations. The variance of S was then calculated at each grid cell from the spread of simulated values. Values and associated uncertainties for the coefficients a_i in equation (2) were estimated by well calibration. Correlation coefficients between V, C and ϕ were evaluated from cross plots of log data upscaled over the reservoir layer.

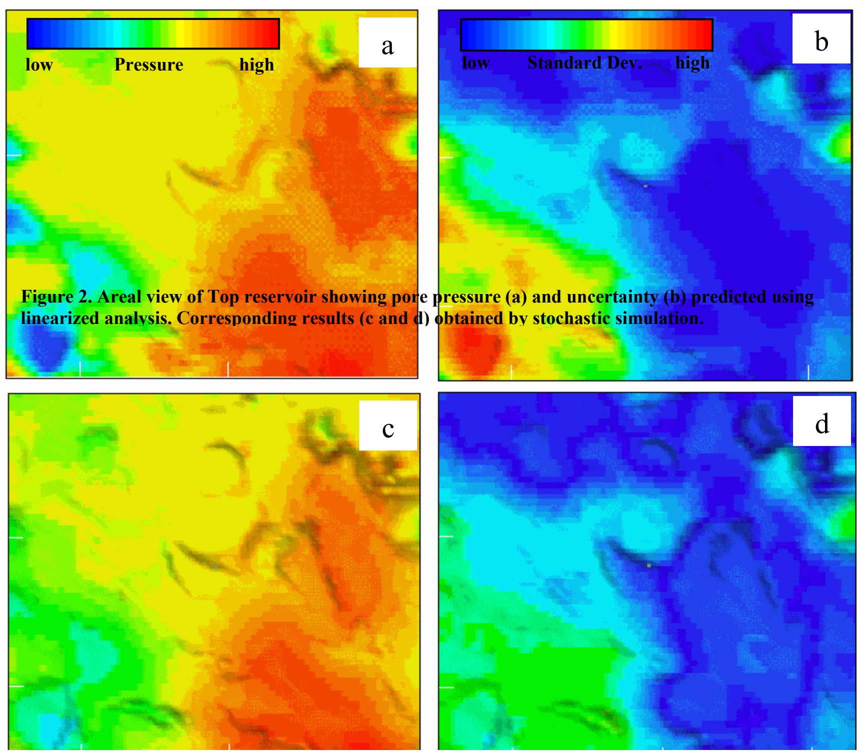

Figure 2. Areal view of Top reservoir showing pore pressure (a) and uncertainty (b) predicted using linearized analysis. Corresponding results (c and d) obtained by stochastic simulation.

Having established PDFs for all the uncertain input variables, pore pressure and uncertainty estimates were calculated using both the linearized approximation and the stochastic approach. The results are presented in Figure 2. Figure 2a shows an areal view of the P predictions at the top of the reservoir obtained using the linearized analysis; i.e., by setting all input variables to their mean values in equation (6). Figure 2b depicts the corresponding uncertainty map calculated from equation (7). For comparison, Figure 2c and 2d show the mean pore pressure and standard deviation map calculated by averaging 500 stochastic simulations. As the simulation scheme fully accounts for nonlinearities in equation (2), it should produce more accurate predictions, especially for statistics impacted by the tails of the local PDFs, which are typically poorly reproduced by the Gaussian assumption made in the linearized scheme. Comparison of Figures 2a-b with 2c-d shows that results from the two methods are broadly similar with the notable exception of the south-western corner, where the linearized calculation produces much lower pressure estimates and higher uncertainty predictions. These discrepancies can be understood by referring to Figure 3, which compares the output PDFs that were calculated by the two methods at one south-western location with high velocity and relatively low pore pressure. The observed bias in the mean pressure calculated in the linear approach stems from the fact that the approximation $E[g(x)] \approx g(\hat{x})$ is poor in the presence of model nonlinearities. The overestimation of the variance by the linearized scheme is explained by the fact that the tails of the Gaussian distribution extend well beyond the hydrostatic and overburden pressure limits. These out-of-range values are automatically rejected in the stochastic simulation, which yields a more narrow range of simulated outcomes and hence a smaller predicted standard deviation. Predictions from the linearized method could be improved by calculating the mean and variance of the Gaussian distribution truncated on the physical pressure limits. However, this correction would not attenuate the bias in the position of the mode of the Gaussian PDF, compared to the histogram of simulated values.

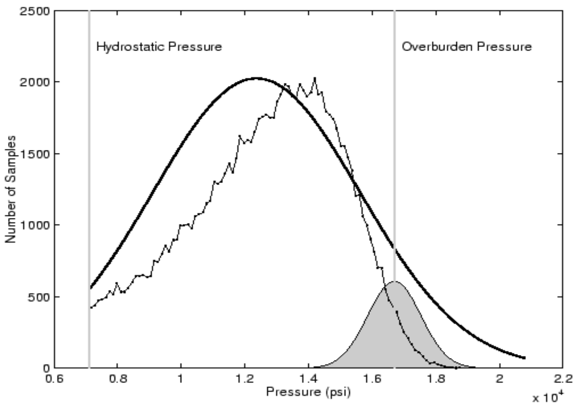

Figure 3. Uncertainty in pore pressure from linearized analysis (thick black line) compared with a histogram of 100,000 samples obtained by simulation, (thin black line). Best estimate from linearized analysis (i.e., mean / mode of Gaussian curve = 12,300 psi) is significantly lower than simulated mean (12,600 psi), indicating nonlinear effects. Standard deviation from linearized analysis (3,300 psi) is much greater than simulated value (2,400 psi) because the Gaussian tails extend well outside the physical limits corresponding to overburden and hydrostatic pressure conditions (grey vertical lines).

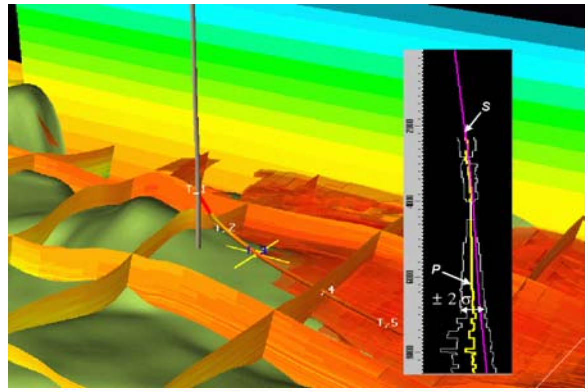

Figure 4. 3-D display of predicted *P* within the reservoir with slice through calculated overburden pressure cube. Well planning with automatic extraction of pore pressure predictions and associated confidence margins may be used to calculate a safe mud weight window. by stochastic simulation.

Conclusions

We have investigated a methodology to propagate uncertainties in seismic pore pressure prediction using a probabilistic 3-D mechanical earth model. PDFs on all input variables such as seismic velocity, porosity, clay volume fraction and overburden pressure are stored as attributes in the 3-D model. An output PDF for pore pressure is then calculated at each point using either a linearized Gaussian calculation or a sequential stochastic simulation approach. The linear scheme is fast and provides an analytical framework for sensitivity analysis by decomposing the pore pressure uncertainty into the sum of the contributions from each uncertain input variable. However, it is not expected to work well when input uncertainties are large relative to the nonlinearities or when estimating statistics that depend on the tails of the output PDFs. While the stochastic approach is slower, it is generally more robust. In particular, it fully captures nonlinearities in the velocity to pressure transform and naturally handles physical limits by rejecting simulated values falling outside the allowed range. In conclusion, the stochastic approach is preferred for quantitative uncertainty assessment but the linearized method remains useful as a first order approximation and for sensitivity analysis. The 3-D P-MEM is particularly useful for assessing risk when planning wells, as shown in Figure 4.

References

Bowers, G.L., Pore pressure estimation from velocity data: Accounting for pore pressure mechanisms besides undercompaction, SPE Drilling and Completion (June 1995) 89-95.

Doyen P.M., den Boer L.D. and Pillet W.R., Seismic porosity mapping in the Ekofisk Field using a new form of collocated cokriging, SPE 36498, 1996.

Plumb, R., Edwards, S., Pidcock, G., Lee, D. and Stacey, B., The mechanical earth model concept and its application to high-risk well construction projects, SPE 59128, 2000.

Granger Morgan, M. and Henrion M., Uncertainty: a guide to dealing with uncertainty in quantitative risk and policy analysis, Cambridge University Press, Cambridge, 1990.

Le Ravalec, M., Noetinger, B. and Hu, L.Y., The FFT Moving Average (FFT-MA) generator: an efficient numerical method for generating and conditioning Gaussian simulations, Mathematical Geology, Vol. 32, pp. 701-723, 2000.

Samson P., Dubrule O. and Euler N., Quantifying the impact of structural uncertainty on gross-rock volume estimates, SPE 35535, 1996.

Sayers, C.M., Smit, T.J.H., van Eden C., Wervelman, R., Bachmann, B., Fitts, T., Bingham, J., McLachlan, K., Hooyman, P., Noeth, S. and Mandhiri, D., Use of reflection tomography to predict pore pressure in overpressured reservoir sands, submitted for presentation at the SEG 2003 annual meeting.

.